Dyes and Pigments 93 (2012) 1401–1407

Contents lists available at SciVerse ScienceDirect

Dyes and Pigments

journal homepage: www.elsevier.com/locate/dyepig

Large fluorescence enhancement of a hemicyanine by supramolecular interaction with cucurbit[6]uril and its application as resettable logic gates

Zhiyong Li [a], Shiguo Sun [a,*], Fengyu Liu [b], Yi Pang [a,c], Jiangli Fan [a], Fengling Song [a], Xiaojun Peng [a,*]

[a] State Key Laboratory of Fine Chemicals, Dalian University of Technology, No. 2 Linggong Road, High-tech District, Dalian 116024, China
[b] State Key Laboratroy of Fine Chemicals, School of Chemistry, Dalian University of Technology, 2 Linggong Road, Ganjingzi District, Dalian 116023, China
[c] Department of Chemistry, The University of Akron, Akron, OH 44325, USA

ARTICLE INFO

Article history:
Received 16 August 2011
Received in revised form
29 September 2011
Accepted 3 October 2011
Available online 15 October 2011

Keywords:
Hemicyanine
Fluorescence enhancement
TICT
Cucurbit[6]uril
Supramolecular chemistry
Logic gate

ABSTRACT

About 270 times fluorescence enhancement was observed when the hemicyanine dye, trans-4-[4-(dimethylamino)styryl]-1-methylpyridinium iodide (DSMI), was included by cucurbit[6]uril (CB[6]). The 1:1 stoichiometry of DSMI/CB[6] complex was determined through optical spectra and ^{1}H NMR measurement. The large fluorescence enhancement was achieved by prohibiting the twisted intramolecular charge transfer (TICT) process of DSMI inside the distorted cavity of CB[6], together with the ion-dipole interaction between DSMI and CB[6]. The distortion of the CB[6] cavity, being as the major reason for the great fluorescence enhancement, was further confirmed in the calculation results. A resettable and reconfigurable logic gate was also constructed with DSMI and CB[6] under different pH situations. This study lays a solid foundation for the design of molecular logic gates by a supramolecular interaction mode.

1. Introduction

Recently, cucurbit[n]urils (CB[n]), [1,2] as rigid host compounds comprised of n glycoluril units linked by pairs of methylene bridges, have been shown to have numerous applications ranging from dye encapsulation, [3] drug delivery, [4] supramolecular catalysis, [5] and enzyme assays [6] to self-assembled molecular devices [7,8]. Because of the negative charge density on the ureido carbonyl groups and the inner surface of the hydrophobic cavity of CB[n]s, small guest molecules may be included through hydrophobic interaction, [9] and binding is possible with metal cations [10,11] and cationic organic molecules via ion-dipole interaction [12–14]. The effect of the supramolecular interaction between CB[n]s and organic dyes such as rhodamine 6G [15,16], neutral red [17] and berberine [18] have been studied [19]. The fluorescence intensity of dyes may be enhanced greatly by binding with CB[n]s, providing the possibility for the designation of molecular logic gates using fluorescence. Thus far, fluorescent logic gates have been constructed by using fluorescent molecular switches based on photoinduced electron transfer (PET), internal charge transfer (ICT), electronic energy transfer (EET), and proton transfer (PT) [20–22]. For most reported studies, however, complicated synthetic processes are required. To replace complicated synthesis, it would be interesting to find a common fluorescent dye which can construct logic gates by host-guest chemistry with CB[n]s. Very recently, Nau [23]illustrated a resettable logic gate using a modular fluorophore-spacer-anchor architecture and CB [7] based on a PET mechanism, where a fluorescence enhancement by a factor of 6–50 was observed. However, it is still a challenge to develop new systems which exhibit much higher signal response to improve switching capability.

To extend our general interest on the supermolecular chemistry of CB[n] [24–28], herein we report the chemically tunable interaction between CB[6] and trans-4-[4-(dimethylamino)styryl]-1-methylpyridinium iodide (DSMI, Fig. 1), a common cationic hemicyanine dye much used as a fluorescence probe for DNA analysis [29], reverse micelles' interface [30] etc. Although the supramolecular interaction between some hemicyanine homologs and CB [7] has been investigated [31,32], the fluorescence of DSMI was found to be increased by as much as 270 times upon binding with CB[6], due to the prohibition of the twisted intramolecular charge transfer (TICT) of the dye in the cavity of CB[6]. Moreover, the fluorescence of DSMI could be modulated by adjusting pH of the solution. All these provided the possibility of producing a logic gate

* Corresponding authors.
E-mail addresses: shiguo@dlut.edu.cn (S. Sun), pengxj@dlut.edu.cn (X. Peng).

0143-7208/$ – see front matter © 2011 Elsevier Ltd. All rights reserved.
doi:10.1016/j.dyepig.2011.10.005

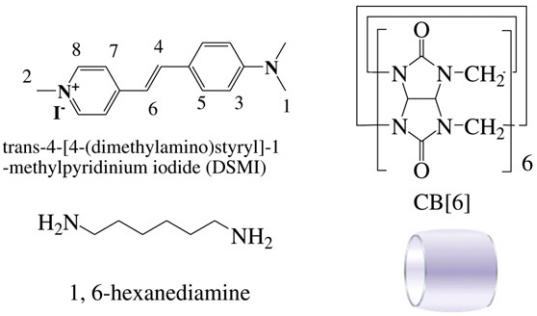

Fig. 1. Structures for DSMI and CB[6] and 1,6-hexanediamine.

with a high fluorescence signal response. In this study, the supramolecular interaction between DSMI and CB[6] was investigated through absorption and fluorescence spectroscopy, ^{1}H NMR, ESI-MS and a computational method, and a resettable and reconfigurable logic gate based on TICT mechanism was constructed by modulating the pH of the solution and adding CB[6] or 1,6-hexanediamine as input signals.

2. Experimental

2.1. Materials and methods

All solvents were of analytical grade and the water used in the test was distilled water. CB[6] and the hemicyanine dye DSMI were synthesized according to the literature [33,34], the purity of CB[6] and DSMI was certified by NMR spectra (DSMI ^{1}H NMR($CDCl_3$, 400 M) δ (ppm): 3.09 (s, 6H), 4.46 (s, 3H), 6.71(d, J = 8.8 HZ, 2H), 6.84(d, J = 16.0 HZ, 1H), 7.53(d, J = 8.8 HZ, 2H), 7.60(d, J = 15.6 HZ, 1H), 7.79(d, J = 7.2 HZ, 2H), 8.78(d, J = 6.8 HZ, 2H); CB[6] ^{1}H NMR(D_2O, 400 M) δ (ppm): 5.73 (d, J = 15.4, 12H), 5.55 (s, 12H), 4.28 (d, J = 16.0, 12H).). 1,6-Hexanediamine of analytic grade was bought from Sinopharm Chemical Reagent Co., Ltd. China and used as received.

NMR data were recorded in D_2O on a Varian Inova-400 spectrometer. Mass spectrometric data were obtained on a Q-TOF mass spectrometer (Micromass, Manchester, England). Absorption spectra were measured on a Perkin–Elmer Lambda 35 UV–Vis spectrophotometer. Fluorescence measurements were performed on a Varian Cary Eclipse Fluorescence Spectrophotometer. The pH titration measurements were made with a Model PHS-3C meter.

The absorption and fluorescence spectra of DSMI with CB[n]s were measured in water. The fluorescence titration experiments were performed as follows: 25 μl of 1.0 × 10^{-3} mol/l stock solution of DSMI and various amount of 2.0 × 10^{-5} mol/L of CB[6] aqueous solution were transferred into a 5 ml volumetric flask, then the volumetric flask was filled to the final volume with distilled water. Fluorescence and absorption spectra were measured after 3 min of ultrasonic agitation. The NMR spectra were obtained in D_2O with DSS (3-(trimethyl-silyl)-1-propanesulfonic acid sodium salt) as internal standard; the protonation form of DSMI was determined by the color of the solution changing from yellow to colorless, and then the pH of the solution was checked by pH test paper.

2.2. Quantum chemistry computational methods

The X-ray structure of CB[6] was used as initial geometry for the calculation [35]. The ONIOM optimization and SP (single-point) Energy were all computed using the Gaussian 09 package [36]. The ONIOM-type approach (oniom(b3lyp/6-31+g:uff)) was adopted according to reference [37], in which the supramolecular complex was divided into two layers: (1) the host, being set as the lower layer, described by a simple molecular mechanics field (UFF), and (2) the guest (DSMI), treated with DFT methodology (B3LYP/6-31G+) as the higher layer. The positions of the host and DSMI were manually set to form at least five different conformations, typically with DSMI partially or fully included by the host cavity. After the host-guest system was optimized to achieve the local energy minimum state, a single-point energy calculation for the inclusion complex was carried out by B3LYP/6-31G+ methods.

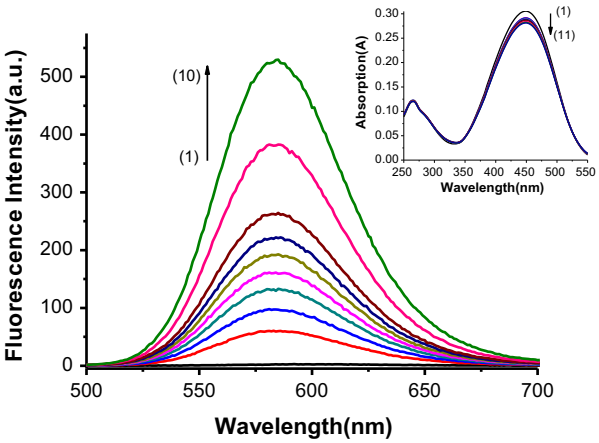

Fig. 2. Fluorescence enhancement with increasing concentration of CB[6], from (1) to (10): 0, 1, 2, 3, 4, 5, 7, 9, 15, 20 μmol. Inset figure is the absorption spectrum decreased with the addition of CB[6]. From (1) to (11): 0, 0.1, 0.2, 0.3, 0.4, 0.5, 0.6, 0.7, 0.8, 0.9, 1.0 equiv of CB[6] was added accordingly, the concentration of dye is 5.0 × 10^{-6} mol/L.

3. Results and discussion

3.1. UV–Vis and fluorescence spectra study

DSMI has an absorption maximum centered at 450 nm and a fluorescence peak at 607 nm in aqueous solution. The absorption maximum peak was observed to be decreased from 0.30 to 0.28 with the addition of 1 equiv. of CB[6] (inset figure of Fig. 2). The significant hypochromicity indicates that the dye is included in CB[6] [18].

The fluorescence response of DSMI increased significantly upon the addition of CB[6] (Fig. 2 and Table 1), and a great enhancement of about 270 times was achieved when 4 equiv. of CB[6] was added into the system. In addition, the fluorescence emission exhibited a blue shift from 607 nm to 582 nm, resulting in a reduced stokes shift (from 141 nm to 109 nm). Previous study [38] has shown that the TICT state dominates the evolution of the excited state of hemicyanine, and the decay is nonradiative [39]. This TICT state is not formed by twisting the dimethylamino group (C–N single bond), but by twisting the entire aniline ring and pyridinium ring (along the C–C single bond of DSMI) [40]. In other words, the

Table 1
Truth table of the AND logic gate based on the emission response of $DSMIH^+$ (5 μM, pH = 2.5) with OH^- and CB[6] as inputs.

I_1[a] CB[6]	I_2[a] OH^-	Output (normalized)[b] If (λ = 582 nm)
0	0	0 (0.003)
1	0	0 (0.025)
0	1	0 (0.017)
1	1	1 (1.000)

[a] OH^- was added until pH 7 is reached, [CB6] = 20 μM.
[b] In parentheses the relative fluorescence intensities are given. The threshold value was settled at 0.1.

formation of the TICT of the hemicyanine is the main pathway for nonradiative decay of DSMI. After the dye was confined in the nonpolar and narrow cavity of CB[6], the rigid environment restricted the rotation of DSMI in the excited state, thereby preventing the formation of TICT and leading to significant fluorescence enhancement. To confirm this speculation, the effects of viscosity and CB[6] on the fluorescence change of DSMI were investigated. Along with the increasing viscosity of the solution, a 91-fold enhancement of the fluorescence intensity and a bathochromic shift on the maximum absorption wavelength from 450 nm to 480 nm were observed concurrently (Figures S1 and S2). This can be ascribed to the increased viscosity causing inhibition of the internal motion around the double bond in the excited state [41]. By contrast, the effect of CB[6] was much larger than that of increased viscosity. In addition, the maximum absorption and emission wavelength of CB[6]/DSMI complex exhibited a hypsochromic shift compared with that under high viscosity condition. When the electron-withdrawing pyridinium group was replaced by a pyridine ring, DSMI, being a typical fluorophore with D-π-A structure, exhibited ca. 100 nm hypsochromic shift of the maximum absorption and emission wavelength, and a 3-fold increase in the fluorescence quantum yield [42]. After the dye was included in the distorted CB[6] cavity [43], the electron-withdrawing ability of the pyridinium ring on DSMI was reduced by the negative charge density on the ureido carbonyl groups of CB[6] through ion-dipole interaction. As a consequence, the absorption and emission peaks exhibited a hypsochromic effect, and the fluorescence intensity was increased significantly. That is to say, the large fluorescence enhancement was achieved by the combination of the confinement on DSMI by the cavity of CB[6] and the ion-dipole interaction between DSMI and CB[6]. The former makes a major contribution to the fluorescence enhancement by prohibiting the TICT process of DSMI.

For the complexation of DSMI and CB[6], the stoichiometry was determined by continuous variation technique (Job-plot) [44] on the basis of the fluorescence intensity of guest DSMI in the presence of CB[6]. The maximum fluorescence was observed at $x = 0.5$ (Figure S3), indicating that the DSMI/CB[6] complex was formed with 1:1 stoichiometry in aqueous solution. Meanwhile, the mass spectrum gave a positively charged peak at m/z 618.2651 (calculated for $[CB[6]/DSMI + H^+]^{2+}$, 618.2286), providing conclusive evidence for the formation of the inclusion complex in 1:1 ratio (Figure S4).

The enhanced fluorescence from the guest (DSMI), upon addition of a non-fluorescent host (CB[6]), is thus attributed to the formation of 1:1 host-guest inclusion complex, and the following equation (1) was utilized to determine the binding constant (K_{eq}) [45].

$$I_f/I_0 = 1 + (I_\infty/I_0 - 1)\frac{K_{eq}[CB[6]]_{eq}}{1 + K_{eq}[CB[6]]_{eq}} \quad (1)$$

where I_∞/I_0 is the fluorescence enhancement when 100% of the dye has been included. I_0 is the fluorescence intensity of DSMI in the absence of CB[6], while I_f is the observed fluorescence intensity at each host molecule concentration tested. K_{eq} is the equilibrium binding constant for the complexation.

The plot in Fig. 3 shows the linear double reciprocal plot of $1/(I_f/I_0 - 1)$ vs. $1/[CB[6]]_0$ ($r = 0.994$), which confirms the 1:1 stoichiometry of the complex (the applicability of equation (1), which will be not linear for higher-order complexes). The binding constant K_{eq} was determined to be 1.02×10^5 L/mol.

The pK_a values of DSMI and DSMI/CB[6] were measured by pH titration based on fluorescence signals. The pK_a of DSMI is 3.1, and a small pK_a shift of 0.8 was found for the inclusion complex (Fig. 4)

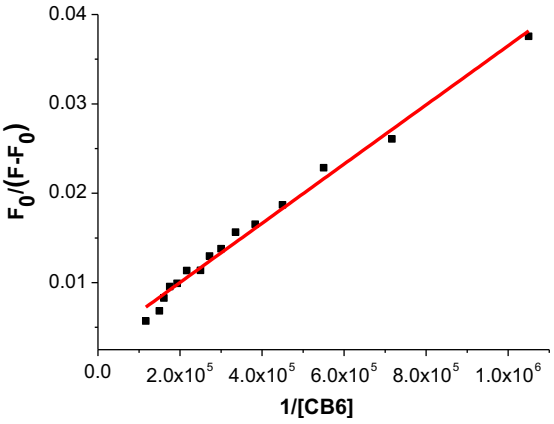

Fig. 3. The double reciprocal plot of the fluorescence titration experiment. The binding constant was determined to be 1.02×10^5 L/mol.

[46]. When the pH of the free and complexed dye solution increased up to the pK_a, the fluorescence of complexed DSMI would switch on while that of free dye still remained off (Fig. 7), providing the possibility of constructing logic gates.

3.2. NMR and computational study

The binding interaction of DSMI and CB[6] was also investigated using ^1H NMR, the chemical shift of each proton being ascertained by ^1H gCOSY measurement (Figure S5). Firstly, the binding stoichiometric ratio between the host and the dye was checked by NMR titration technology. Proportional dyes dissolved in D_2O were added into the saturated solution of CB[6] in D_2O to get the different NMR spectra as shown in Figures S6 and S7. When the CB[6]/dye ratio was larger than 1, the proton signals did not shift further. Moreover, the proton signals for the methine group of CB[6] shifted upfield with the addition of dyes until the dye/CB[6] ratio was larger than 1. All these results implied the formation of 1:1 dye/CB[6] complexes. Then, the binding position of the CB[6] and the dyes was investigated by comparison of the proton signals. As shown in Fig. 5, when 1.0 equiv. CB[6] was added into the aqueous solution of DSMI, complexation with CB[6] shifted the H2, H4, H6, H7 and H8 signals significantly upfield, while H3 and H5 signals were almost unchanged. In sharp contrast, H1 signals were shifted

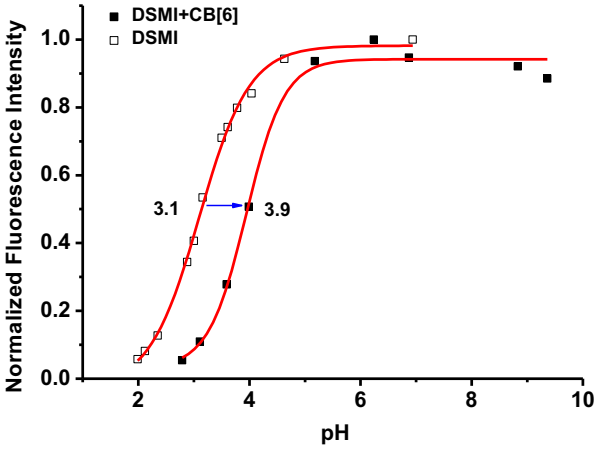

Fig. 4. pKa shift of DSMI upon complexation by CB[6] monitored through the fluorescence change upon pH variation for the free dye DSMI and the DSMI/CB[6] complex ($\lambda_{ex} = 450$ nm, $\lambda_{em} = 582$ nm).

downfield. These signal changes, in conjunction with relevant reports [47–49], led us to the conclusion that the double bonds, pyridine ring and the *N*-methyl on the pyridine ring were included in the cavity of CB[6] as illustrated in Fig. 6. To determine the binding mode of the protonated form of DSMI (DSMIH$^+$), the ^{1}H NMR spectrum of DSMIH$^+$ was obtained by adding deuterium HCl to the dye solution until the solution colour changed from yellow to colorless (Fig. 5(d)). Then 1 equiv. CB[6] was added to get Fig. 5(c). The chemical shift of H2, H4, H5, H6, H7 and H8 moved upfield dramatically, while that of H1 shifted negligibly and H3 moved downfield. The upfield-shifted signals indicated that the proton on the left of H3 were all shielded by CB[6]. Comparing with the NMR spectra of DSMI, it is easy to get the conclusion that the CB[6] cavity shift to the aniline ring to shield H5 when the dye is protonated.

The doublets of CB[6] at 4.06 and 5.49 ppm split into two doublets respectively (Fig. 5(e)) in the case of DSMIH$^+$ and CB[6], suggesting that the two portals are no longer in equivalent environments after inclusion.

3.3. Quantum chemistry calculation

Computational methods were used to gain further insight into the geometry and the nature of interaction of DSMI with the host CB[6]. As the host/DSMI complex is too large for *ab initio* calculation, therefore, an ONIOM-type approach (oniom(b3lyp/6-31+g:uff)) was adopted. The calculation result showed significant energy differences for movement of CB[6] along the DSMI molecule (Figure S8). The complex energy reached a minimum when CB[6] rested over the pyridinium ring as shown in Fig. 6a and b, which is in good agreement with the NMR results. The distortion of CB[6] cavity could be clearly observed under this condition, which coincides well with the X-ray single crystal structure of distorted CB[6] caused by the 4-methylpyridinium cation [43]. The energy of the complex is shown in Table S1, and the largest binding energy (BE) was calculated to be −84.2 kcal/mol.

A similar method was used to calculate the geometry optimization and binding energy of the DSMIH$^+$/CB[6] complex. As shown in Table S2, the binding energy is −87.4 kcal/mol, which is larger than that of the DSMI/CB[6] complex. The stable conformation is illustrated in Fig. 6c and d, where CB[6] remained over the pyridinium ring. However, the binding energy was decreased to −82.03 kcal/mol when CB[6] resided on the aniline ring part of the molecule (Figure S9). The energy difference between the two conformations is only 5.3 kcal/mol, while, in the case of DSMI/CB[6], the energy difference for the two conformations is 33.9 kcal/mol. The small energy difference between the two conformations of DSMIH$^+$/CB[6] illustrates the possibility that CB[6] can move from the pyridinium ring to the aniline ring after protonation. However, the two methyl groups were no longer coplanar with the benzene ring. This steric hindrance somehow prohibited the complete inclusion of the aniline ring inside CB[6], leading to only aniline H5 being shielded as demonstrated in the NMR results.

3.4. Logic gates construction

The favorable fluorescence characteristics of DSMI in its uncomplexed and CB[6]-complexed forms at different pH values allow the construction of a binary off-on hemicyanine fluorescence switching for molecular logic, i.e., assignment of 0 and 1 for off and on fluorescence output, respectively (Fig. 7).

The relevant situation for fluorescence switching at pH = 2.5 and 7 is illustrated in Scheme 1. Considering 5 μM DSMI at pH = 2.5 in the absence of CB[6] as initial state (left), addition of CB[6] can be taken as input 1 (I_1), while addition of base (OH^-) as input 2 (I_2). The initial state (left), composed of the protonated form of DSMI, has a low fluorescence and characterizes the output as off (binary

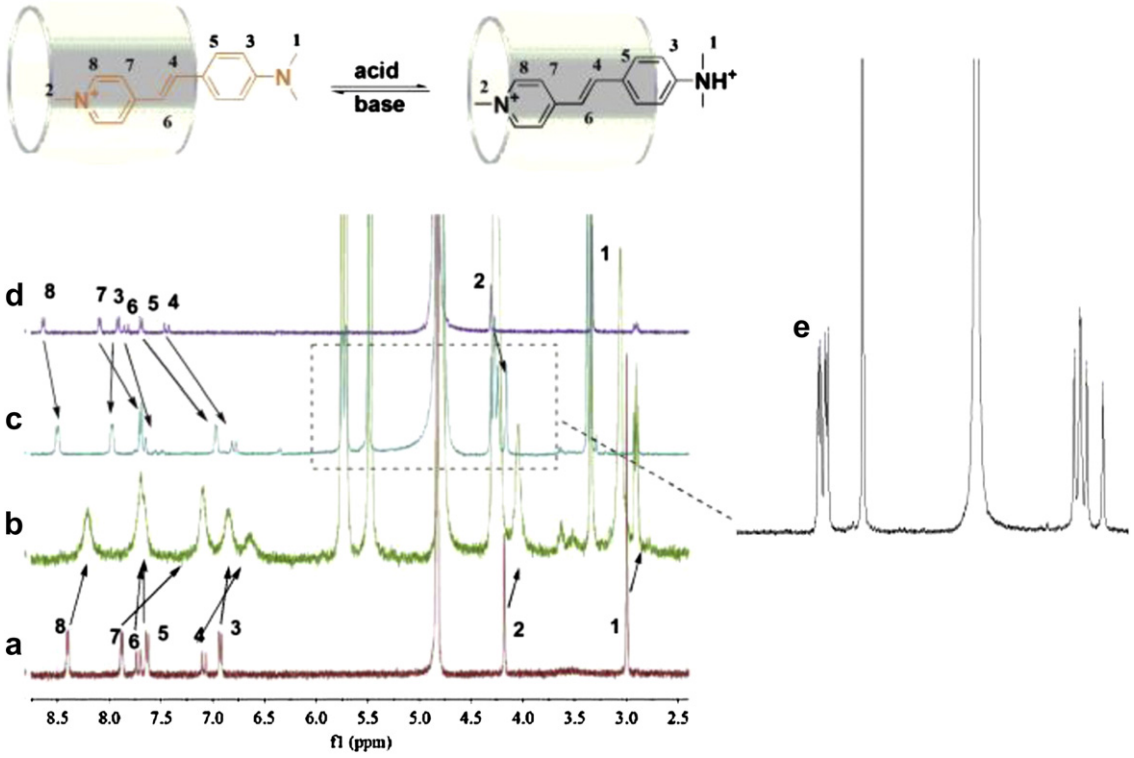

Fig. 5. ^{1}H NMR titration of CB[6] to DSMI and DSMIH$^+$ (D_2O, 400 MHz), (a) 0 and (b) 1 equiv. of CB[6] was added to DSMI, (c) 1 and (d) 0 equiv. of CB[6] was added to DSMIH$^+$. (e) the enlarged curve of CB[6] part in curve c. the concentration of DSMI and DSMIH$^+$ is 2.7 mM (0.5 mg of dye was added to 0.5 ml D_2O).

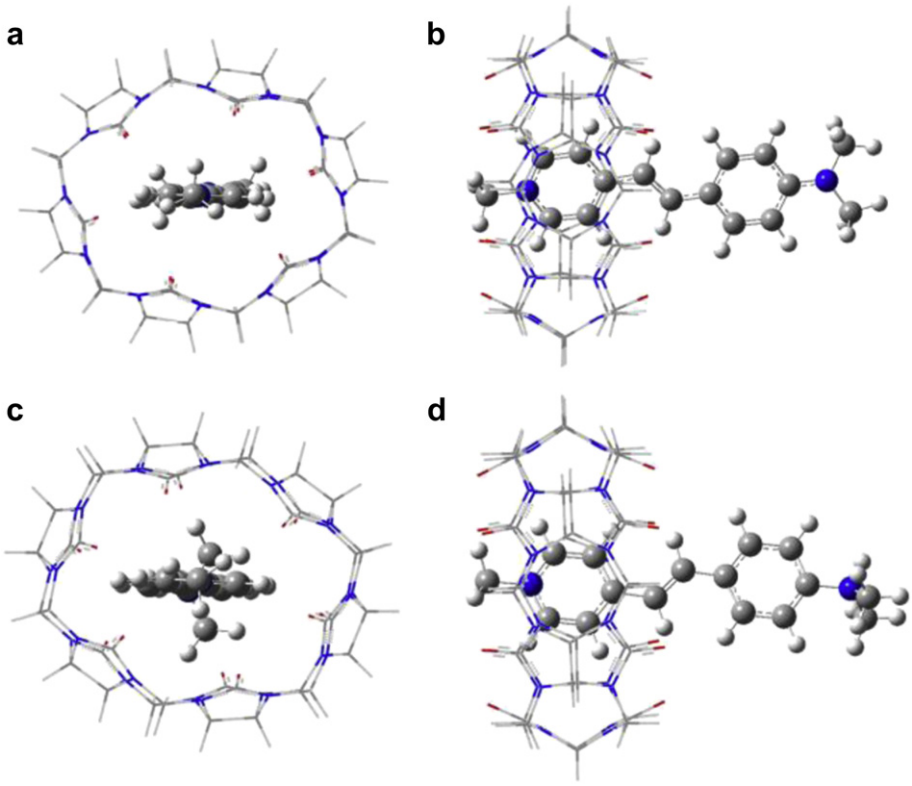

Fig. 6. Minimized structure of the CB[6] complex with DSMI (a, b) and $DSMIH^+$(c, d) viewed from front (a, c) and side (b, d). The binding energy obtained using B3LYP/6–31G + method is −84.2 and −87.4 kcal/mol respectively.

0). For an addition of a single input, either CB[6] (20 μM) or OH^-, the fluorescence output remains off (binary 0). The fluorescence of DSMI itself is also very low, corresponding with the binary 0. Addition of CB[6] alone does not result in any strong fluorescence emission, due to the protonated conformation of DSMI/CB[6] complex exhibiting low fluorescence. It is the combination of deprotonation and complexation that switches the fluorescence output on (right state), and this can only be achieved by the simultaneous presence of both inputs. Hence, the system can be used to mimic the function of an AND logic gate with supramolecular input (Table 1).

It is highly desirable to design reconfigurable and resettable logic gates by chemical manipulations. For instance, chemically-driven logic gates, acid–base neutralization [50] or metal-ion decomplexation by chelators [51] have been demonstrated as resetting. Similarly, host-guest complexes provide another possibility through the addition of a competitive guest to reset the molecular logic gates [52]. To prove this, 20 μM of 1,6-hexanediamine ($Ka = (4.49 \pm 0.84) \times 10^8\ M^{-1}$ at pH = 4.5) [53], which is known to bind very strongly with CB[6], was employed at pH = 7 to displace DSMI from its CB[6] complex (Reset 2 in Scheme 1). The OH^- input, as used in the AND logic gate discussed, was reset by the conventional proton neutralization (Reset 1 in Scheme 1). That is to say, simultaneous decomplexation and protonation restores the initial status (left state in Scheme 1). Therefore, this system is a naturally reconfigurable logic gate as the reset processes are precisely NOT and NOR logic gates. The binding interaction of DSMI with CB[6] led to the fluorescent DSMI/CB[6] complex at pH = 7 in solution, forming the initial logical molecule device. We can then add either protons or 1,6-hexanediamine as input (binary 1). When the pH of the solution was modulated to 2.5, the non-fluorescent $DSMIH^+$/CB[6] complex was formed to produce the output 0. When the 1,6-hexanediamine was added, the fluorescent DSMI/CB[6] complex would be replaced by the non-fluorescent 1,6-hexanediamine/CB[6] complex and uncomplexed DSMI, which then gave the output 0 as well. The fluorescence curves of different states are shown in Fig. 7. Consequently, these translate into NOT logic gates. Combination of the two logic gates yielded a NOR logic gate. On the other hand, when the free DSMI was set as initial state, protonation of DSMI quenched the weak fluorescence. Binding of

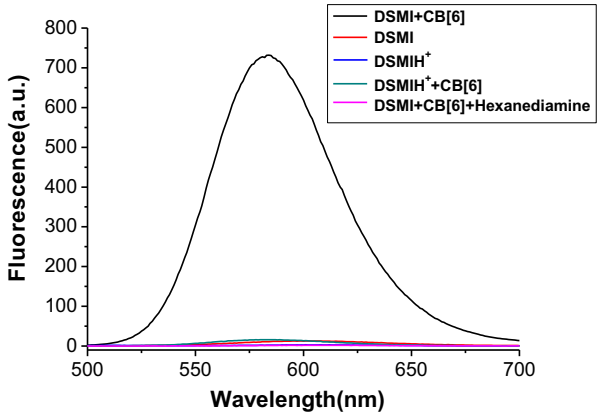

Fig. 7. The fluorescence curves at different states of the logic gate: a) DSMI at pH = 2.5 without CB[6] (blue), b) DSMI at pH = 2.5 with CB[6] (cyan), c) DSMI at pH = 7.0 without CB[6] (red), d) DSMI at pH = 2.5 with CB[6] (black), e) the solution of CB[6] and DSMI with the addition of 1,6-hexanediamine at pH = 7.0. The concentration of DSMI, CB[6] and 1,6-hexanediamine is 5 μM, 20 μM and 20 μM respectively. (For interpretation of the references to colour in this figure legend, the reader is referred to the web version of this article.)

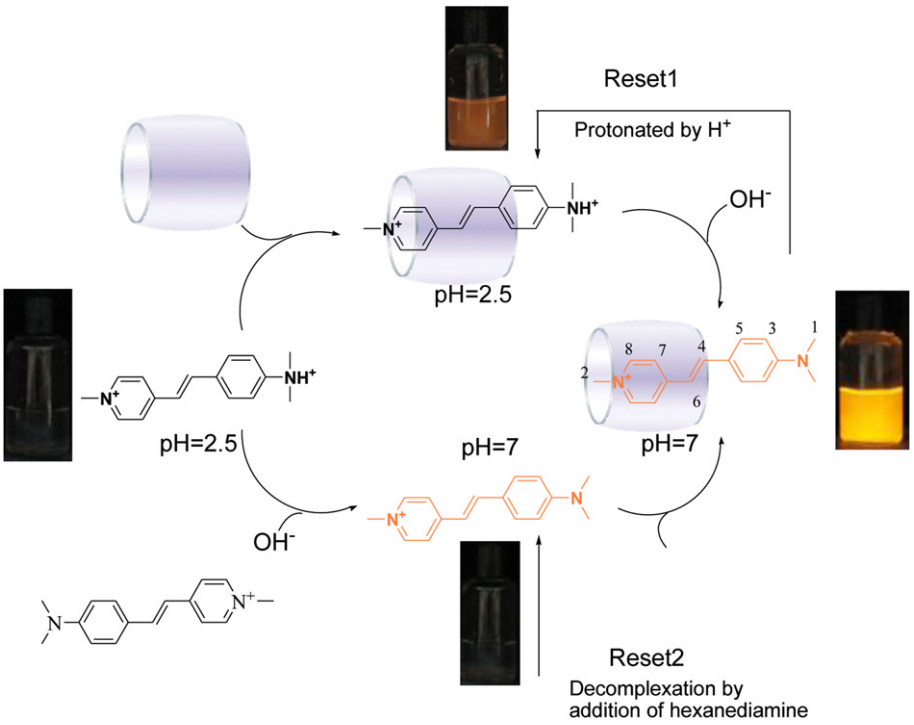

Scheme 1. The schematic operating process of the resettable AND logic gate.

CB[6], in turn, increased the fluorescence quantum yield. Combinational effect of binding with CB[6] and protonation resulted in fluorescence quenching. This behavior is equivalent to the INHIBIT logic gate. The truth table of these reconfigurable logic gates is shown in Table S3.

4. Conclusion

In summary, a large fluorescence enhancement of DSMI was realized by the formation of an inclusion complex with CB[6], and the distorted cavity of CB[6] was observed in computational results. The distorted cavity of CB[6], which exhibited inhibition of the TICT process by restricting the rotation of the aniline ring and pyridinium ring of DSMI, seems to be the main reason for the large increase in fluorescence. Meanwhile, the ion-dipole interaction between DSMI and CB[6] may make a minor contribution to the fluorescence enhancement. A reconfigurable and resettable molecular logic gate system was constructed by modulating the pH of the solution and adding CB[6] to or removing it from the hemicyanine dye. This study laid a solid foundation for the design of molecular logic gates by a supramolecular interaction mode.

Acknowledgments

This work was financially supported by State Key Laboratory of Fine Chemicals (KF0909), Dalian University of Technology, the Education Ministry and National Natural Science Foundation of China (Nos. 21072024, 20872012, 707016, 20706008, 20725621), Specialized Research Fund for the Doctoral Program of Higher Education (No. 200801411004), the Open Research Fund of State Key Laboratory of Bioelectronics, Southeast University, China Postdoctoral Science Foundation (No. 20100471434) and National Basic Research Program of China (2009CB724700).

Appendix. Supplementary material

Electronic Supplementary Information (ESI) available: absorption, fluorescence spectra, Job-Plot, ^{1}H gCOSY NMR, ESI-MS, more detailed computational results and the truth table of the reconfigurable logic gate. See doi:10.1016/j.dyepig.2011.10.005.

References

[1] Lagona J, Mukhopadhyay P, Chakrabarti S, Isaacs L. The cucurbit[n]uril family. Angew Chem Int Ed 2005;44(31):4844–70.
[2] Lee JW, Samal S, Selvapalam N, Kim HJ, Kim K. Cucurbituril homologues and derivatives: new opportunities in supramolecular chemistry. Acc Chem Res 2003;36(8):621–30.
[3] Koner AL, Nau WM. Cucurbituril encapsulation of fluorescent dyes. Supramol Chem 2007;19(1–2):55–66.
[4] Angelos S, Khashab NM, Yang YW, Trabolsi A, Khatib HA, Stoddart JF, et al. pH clock-operated mechanized nanoparticles. J Am Chem Soc 2009;131(36):12912–4.
[5] Basilio N, Garcia-Rio L, Moreira JA, Pessego M. Supramolecular catalysis by cucurbit[7]uril and cyclodextrins: similarity and differences. J Org Chem 2010;75(3):848–55.
[6] Hennig A, Bakirci H, Nau WM. Label-free continuous enzyme assays with macrocycle-fluorescent dye complexes. Nat Methods 2007;4(8):629–32.
[7] Zou DP, Andersson S, Zhang R, Sun SG, Akerrnark B, Sun LC. A host-induced intramolecular charge-transfer complex and light-driven radical cation formation of a molecular triad with cucurbit[8]uril. J Org Chem 2008;73(10):3775–83.
[8] Liu JJ, Xu Y, Li XC, Tian H. Synthesis and characteristics of a novel pseudorotaxane with the diarylethene as the functional stopper. Dyes Pigm 2008;76(1):294–8.
[9] Wyman IW, Macartney DH. Cucurbit[7]uril host-guest complexes with small polar organic guests in aqueous solution. Org Biomol Chem 2008;6(10):1796–801.
[10] Whang D, Heo J, Park JH, Kim K. A molecular bowl with metal ion as bottom: reversible inclusion of organic molecules in cesium ion complexed cucurbituril. Angew Chem Int Ed 1998;37(1–2):78–80.
[11] Liu JX, Long LS, Huang RB, Zheng LS. Interesting anion-inclusion behavior of Cucurbit[5]uril and its lanthanide-capped molecular capsule. Inorg Chem 2007;46(24):10168–73.
[12] Marquez C, Hudgins RR, Nau WM. Mechanism of host-guest complexation by cucurbituril. J Am Chem Soc 2004;126(18):5806–16.

[13] Wang RB, Yuan L, Macartney DH. A green to blue fluorescence switch of protonated 2-aminoanthracene upon inclusion in cucurbit[7]uril. Chem Commun 2005;(47):5867–9.
[14] Gromov SPV, Artem I, Kuz'mina Lyudmila G, Kondratuk Dmitry V, Sazonov Sergey K, Strelenko, Yuri A, Alfimov Michael V, Howard Judith AK. Photocontrolled molecular assembler based on cucurbit[8]uril: [2+2]-Autophotocycloaddition of styryl dyes in the solid state and in water. Eur J Org Chem 2010;2010(13):2587–99.
[15] Mohanty J, Nau WM. Ultrastable rhodamine with cucurbituril. Angew Chem Int Ed 2005;44(24):3750–4.
[16] Mohanty J, Pal H, Ray AK, Kumar S, Nau WM. Supramolecular dye laser with cucurbit[7]uril in water. Chemphyschem 2007;8(1):54–6.
[17] Mohanty J, Bhasikuttan AC, Nau WM, Pal H. Host-guest complexation of neutral red with macrocyclic host molecules: contrasting pK(a) shifts and binding affinities for cucurbit[7]uril and beta-cyclodextrin. J Phys Chem B 2006;110(10):5132–8.
[18] Megyesi M, Biczok L, Jablonkai I. Highly sensitive fluorescence response to inclusion complex formation of berberine alkaloid with cucurbit[7]uril. J Phys Chem C 2008;112(9):3410–6.
[19] Nau WM, Mohanty J. Taming fluorescent dyes with cucurbituril. Int J Photoenerg 2005;7(3):133–41.
[20] Pischel U. Chemical approaches to molecular logic elements for addition and subtraction. Angew Chem Int Ed 2007;46(22):4026–40.
[21] Szacilowski K. Digital information processing in molecular systems. Chem Rev 2008;108(9):3481–548.
[22] Andreasson J, Pischel U. Smart molecules at work-mimicking advanced logic operations. Chem Soc Rev 2010;39(1):174–88.
[23] Pischel U, Uzunova VD, Remon P, Nau WM. Supramolecular logic with macrocyclic input and competitive reset. Chem Commun 2010;46(15):2635–7.
[24] Sun SG, Zhang R, Andersson S, Pan JX, Akermark B, Sun LC. The photoinduced long-lived charge-separated state of Ru(bPY)(3)-methylviologen with cucurbit[8]uril in aqueous solution. Chem Commun 2006;(40):4195–7.
[25] Sun SG, Andersson S, Zhang R, Sun LC. Unusual partner radical trimer formation in a host complex of cucurbit[8]uril, ruthenium(II) tris-bipyridine linked phenol and methyl viologen. Chem Commun 2010;46(3):463–5.
[26] Zhang TY, Sun SG, Liu FY, Fan JL, Pang Y, Sun LC, et al. Redox-induced partner radical formation and its dynamic balance with radical dimer in cucurbit[8]uril. Phys Chem Chem Phys 2009;11(47):11134–9.
[27] Zhang TY, Sun SG, Liu FY, Pang Y, Fan JL, Peng XJ. Interaction of DNA and a series of aromatic donor-viologen acceptor molecules with and without the presence of CB[8]. Phys Chem Chem Phys 2011;13(20):9789–95.
[28] Sun SG, Gao WY, Liu FY, Li FS, Fan JL, Peng XJ. Redox-induced Ru(bpy)(3)(2+) -methylviologen radical formation and its dimerization in cucurbit[8]uril. Phys Chem Chem Phys 2011;13(2):570–5.
[29] Kumar CV, Turner RS, Asuncion EH. Groove binding of a styrylcyanine dye to the DNA double Helix – the salt effect. J Photochem Photobiol A 1993; 74(2–3):231–8.
[30] Moyano F, Quintana SS, Falcone RD, Silber JJ, Correa NM. Characterization of multifunctional reverse micelles' interfaces using hemicyanines as molecular probes. I. Effect of the hemicyanines' structure. J Phys Chem B 2009;113(13): 4284–92.
[31] Fedorova OA, Chernikova EY, Fedorov YV, Gulakova EN, Peregudov AS, Lyssenko KA, et al. Cucurbit[7]uril complexes of crown-ether derived styryl and (Bis)styryl dyes. J Phys Chem B 2009;113(30):10149–58.
[32] Zhang HY, Wang QC, Liu MH, Ma X, Tian H. Switchable V-type [2]pseudorotaxanes. Org Lett 2009;11(15):3234–7.
[33] Day A, Arnold AP, Blanch RJ, Snushall B. Controlling factors in the synthesis of cucurbituril and its homologues. J Org Chem 2001;66(24):8094–100.
[34] Huang YY, Cheng TR, Li FY, Huang CH, Hou TJ, Yu AC, et al. Photophysical studies on the mono- and dichromophoric hemicyanine dyes I. Photoelectric conversion from the dye modified ITO electrodes. J Phys Chem B 2002; 106(39):10020–30.
[35] Dybtsev DN, Gerasko OA, Virovets AV, Sokolov MN, Fedin VP. Unexpected guest-controlled formation of two-layered structure in supramolecular adduct of [W3S4(H2O)(9)](4+) and cucurbituril. Inorg Chem Commun 2000; 3(7):345–9.
[36] Frisch MJ, Trucks GW, Schlegel HB, Scuseria GE, Robb MA, Cheeseman JR, et al. Gaussian 09, Revision A02. Wallingford CT: Gaussian, Inc; 2009.
[37] Gadde S, Batchelor EK, Weiss JP, Ling YH, Kaifer AE. Control of H- and J-aggregate formation via host-guest complexation using cucurbituril hosts. J Am Chem Soc 2008;130(50):17114–9.
[38] Huang YY, Cheng TR, Li FY, Luo CP, Huang CH, Cai ZG, et al. Photophysical studies on the mono- and dichromophoric hemicyanine dyes II. Solvent effects and dynamic fluorescence spectra study in chloroform and in LB films. J Phys Chem B 2002;106(39):10031–40.
[39] McHale JL. Subpicosecond solvent dynamics in charge-transfer transitions: opportunities in resonance Raman spectroscopy. Acc Chem Res 2001;34(4): 265–72.
[40] Cao X, Tolbert RW, McHale JL, Edwards WD. Theoretical study of solvent effects on the intramolecular charge transfer of a hemicyanine dye. J Phys Chem A 1998;102(17):2739–48.
[41] Turkewitsch P, Darling GD, Powell WS. Enhanced fluorescence of 4-(p-dimethylaminostyryl)pyridinium salts in the presence of biological macromolecules. J Chem Soc Faraday Trans 1998;94(15):2083–7.
[42] Wang WL, Helgeson R, Ma B, Wudl F. Synthesis and optical properties of cross-conjugated bis(dimethylaminophenyl)pyridylvinylene derivatives. J Org Chem 2000;65(18):5862–7.
[43] Samsonenko DG, Virovets AV, Lipkowski J, Geras'ko OA, Fedin VP. Distortion of the cucurbituril molecule by an included 4-methylpyridinum cation. J Struct Chem 2002;43(4):664–8.
[44] Connors KA. Binding constants: the measurement of molecular complex Stability. New York: Wiley; 1997.
[45] Zhou YY, Yu HP, Zhang L, Sun JY, Wu L, Lu Q, et al. Host properties of cucurbit [7] uril: fluorescence enhancement of acridine orange. J Incl Phenom Macrocycl Chem 2008;61(3–4):259–64.
[46] Saleh N, Koner AL, Nau WM. Activation and stabilization of drugs by supramolecular pK(a) shifts: drug-delivery applications tailored for cucurbiturils. Angew Chem Int Ed 2008;47(29):5398–401.
[47] Kim Y, Kim H, Ko YH, Selvapalam N, Rekharsky MV, Inoue Y, et al. Complexation of aliphatic ammonium ions with a water-soluble cucurbit[6] uril derivative in pure water: isothermal calorimetric, NMR, and X-ray crystallographic study. Chem Eur J 2009;15(25):6143–51.
[48] Mohanty J, Bhasikuttan AC, Choudhury SD, Pal H. Noncovalent interaction of 5,10,15,20-tetrakis(4-N-methylpyridyl)porphyrin with cucurbit[7]uril: a supramolecular architecture. J Phys Chem B 2008;112(35):10782–5.
[49] Ling YH, Mague JT, Kaifer AE. Inclusion complexation of diquat and paraquat by the hosts cucurbit[7]uril and cucurbit[8]uril. Chem Eur J 2007;13(28): 7908–14.
[50] Margulies D, Melman G, Shanzer A. Fluorescein as a model molecular calculator with reset capability. Nat Mater 2005;4(10):768–71.
[51] Guo ZQ, Zhu WH, Shen LJ, Tian H. A fluorophore capable of crossword puzzles and logic memory. Angew Chem Int Ed 2007;46(29):5549–53.
[52] Praetorius A, Bailey DM, Schwarzlose T, Nau WM. Design of a fluorescent dye for indicator displacement from cucurbiturils: a macrocycle-responsive fluorescent switch operating through a pK(a) shift. Org Lett 2008;10(18): 4089–92.
[53] Liu SM, Ruspic C, Mukhopadhyay P, Chakrabarti S, Zavalij PY, Isaacs L. The cucurbit[n]uril family: prime components for self-sorting systems. J Am Chem Soc 2005;127(45):15959–67.